Contents lists available at ScienceDirect

Applied Catalysis B: Environmental

NO reduction by CO over gold catalysts supported on Fe-loaded ceria

L. Ilieva [a,*], G. Pantaleo [b,**], N. Velinov [a], T. Tabakova [a], P. Petrova [a], I. Ivanov [a], G. Avdeev [c], D. Paneva [a], A.M. Venezia [b]

[a] Institute of Catalysis, Bulgarian Academy of Sciences, 1113 Sofia, Bulgaria
[b] Istituto per lo Studio di Materiali Nanostrutturati, CNR, I-90146 Palermo, Italy
[c] Institute of Physical Chemistry, Bulgarian Academy of Sciences, 1113 Sofia, Bulgaria

ARTICLE INFO

ABSTRACT

Nanosized gold catalysts on Fe-loaded ceria were studied in NO reduction by CO in the presence of H_2 and water. The Fe-modified ceria supports (5, 10 and 20 wt% Fe_2O_3) were synthesized by two different methods: mechanochemical mixing (MM) and impregnation (IM) methods. Gold (3 wt%) was loaded by deposition-precipitation method. The samples was characterized by XRD and H_2-TPR measurements; Mössbauer spectroscopy results of fresh and used catalysts were used for clarifying the role of Fe addition. It was established that the presence of very small gold particles was not of crucial importance. The Fe-modification of ceria was beneficial for NO conversion, however it decreased the selectivity to N_2 by increasing the selectivity to N_2O. The 100% selectivity to N_2 at 250 °C as well as a high catalytic activity and stability was observed over gold catalyst on ceria support containing 5 wt% Fe_2O_3 and prepared by IM method.

1. Introduction

The removal of nitrogen oxides from combustion exhausts has a beneficial impact on the environment, since it decreases the formation of acid rain and photochemical smog. Concerning the mobile sources, one of the ways of $DeNO_x$ is the catalytic reduction by hydrocarbons or by CO. The use of CO as a reducing agent has advantages for practical application: (i) because of its presence in significant amounts in automobile exhausts – CO often occurs due to ineffective combustion processes and generally the concentration of CO in the exhaust gas is greater than that of H_2 by about 10 times; (ii) CO is an important source of urban air pollution and the reduction of NO_x by CO to N_2 and CO_2 leads to CO emissions abatement as well. The problem with the exhaust gases of engines operating under conditions around the stoichiometric air to fuel ratio, maintaining the amount of supplied air on a level just

sufficient for the complete combustion of the fuel, has been solved using metal oxide supported platinum group metals for NO_x reduction (the conventional tree-way catalysts (TWC)). The present TWC are able to remove the exhaust NO_x with engines operating close to stoichiometric conditions. However, TWC cannot effectively remove harmful emissions from cars during the first several minutes of driving. During this "cold start" period, i.e., before the light-off of the monolith, the low temperature of the catalytic surface causes too slow reaction kinetics to achieve a full conversion, resulting in a major contribution to air pollution. One drawback is represented by the incomplete reduction of NO into the undesirable green-house gas N_2O. Stringent regulation requires more efficient metal catalysts which are able to convert NO to N_2 selectively (Eq. (1)) during the "cold start" regime and/or to enhance the reaction $N_2O + CO$ according to the Eq. (3).

$$2CO + 2NO \rightarrow N_2 + 2CO_2 \tag{1}$$

$$CO + 2NO \rightarrow N_2O + CO_2 \tag{2}$$

$$N_2O + CO \rightarrow N_2 + CO_2 \tag{3}$$

Additionally, a low temperature catalytic activity is needed for the "idling" phase when the engine operates under prolonged idling conditions. Thus the gold based catalysts could play a role in the future to enhance the performance of the TWC in the low temperature range which is still a hot topic. In the book "Gold: Science

and Applications" the authors envisaged a relatively simple system in which PGM- and gold-based catalysts operate in parallel or sequentially. The gold catalyst is in use at low temperatures and it is bypassed in favor of the PGM catalyst at higher temperatures. Other possibility is using the gold catalyst at relatively low temperatures in a second exhaust box. In this way, maximum conversion activity could be maintained both at low temperatures using the gold based system and at high temperatures using the PGM TWC [[1] and references therein].

The reported results about supported nanosized gold catalysts for NO_x reduction by H_2, CO or hydrocarbons [2–8] are promising especially for the "cold start" phase in view of the observed low temperature activity. Generally, the most studied component of the TWC has been cerium oxide [9] since it is able to stabilizes the dispersion of noble metals and it stores and releases oxygen. Some of us reported results on the reduction of NO with CO over gold deposited on synthesized by co-precipitation ceria modified with Al [10] or RE (RE = Y, La, Sm and Gd) [11] as well as on Al- and RE-doped ceria prepared by mechanochemical mixing [12,13]. The modification of ceria with alumina decreased the activity, but Al acts as a structural promoter, which prevents the agglomeration both of gold and ceria particles during the catalytic operation. Experiments with hydrogen addition were carried out because hydrogen is included in automotive exhaust gas stream mainly due to the water gas shift (WGS) reaction (the exhaust gases contain permanently 10–12% H_2O) and/or by steam reforming [3]. It has been shown that the addition of hydrogen to the feed strongly enhanced both the NO and CO conversions [10,14]. Concerning the role of water to improve the NO reduction it is suggested that when CO is converted to CO_2 through the WGS reaction, the produced hydrogen acts as a very effective reductant for NO_x removal [15]. In our previous investigation we also connected the effect of water to the hydrogen produced by WGSR, however H_2 was not effective reducing agent but strongly enhanced both the NO and CO conversions keeping the ceria surface reduced [12,13]. Studying the NO + CO reaction in the presence or in the absence of H_2 over gold on ceria and ceria–alumina mixed supports by FTIR spectroscopy, Kantcheva et al. [16] have established that the presence of oxygen vacancies at ceria surface helps in the dissociation of NO to nitrogen and oxygen species. Nanosized gold improved the reducibility of ceria surface layers. The proposed role of hydrogen for enhancing the NO and CO conversion was indirect, in the sense of keeping the catalyst surface, particularly the CeO_2, reduced during the course of the reaction.

The formation of ammonia during the catalytic NO removal from the automobile exhaust is well documented as a principal problem in the design of catalysts for controlling exhaust gases [17]. Very promising results for the selectivity toward N_2 were achieved using the RE as dopants because in the presence of water no NH_3 and no CH_4 was recorded within the whole temperature interval up to 400 °C (N_2O was observed bellow 150 °C) [11,13].

The nature of dopant plays an important role for ceria modification. Gupta et al. [18] have studied by DFT calculations the effect of transition metal ion (Me = Mn, Fe, Co, Ni) and rare earth ion (RE = Y, La) substitution in ceria structure. They have established that the transition metal doping results in a higher effect in improving the OSC of ceria because of formation of longer Ce—O bonds. Ueda and Haruta [3] have reported that oxides containing iron provide the highest catalytic activity in the NO + CO reaction. The listed results motivated the present investigation, focused on the catalytic behavior in the NO reduction by CO (in the presence of H_2 and water) over nanosized gold catalysts on Fe-loaded ceria. The catalytic activity and selectivity was compared. The effect of the preparation method of the mixed supports (mechanochemical mixing or impregnation) and the amount of Fe_2O_3 was revealed. A special attention was paid on the role of the separate Fe_2O_3 phase

by means of Mössbauer measurements of fresh and used gold catalysts.

2. Experimental

2.1. Sample preparation

Two different methods, in particular impregnation (IM) and mechanochemical mixing (MM), were used for preparation of Fe-modified ceria supports (5, 10 and 20 wt% Fe_2O_3). The impregnation was carried out by stirring of ceria in aqueous solution of $Fe(NO_3)_3 \cdot 9H_2O$ at room temperature for 4 h, evaporation under vacuum at 70 °C in a rotary evaporator until complete removal of water and calcination in air at 400 °C for 2 h. Ceria was laboratory-made by precipitation of aqueous solution of $Ce(NO_3)_3 \cdot 6H_2O$ with K_2CO_3 at constant pH 9.0 and at a temperature of 60 °C, aging at the same temperature for 1 h, filtering and washing until no NO_3^- ions could be detected; drying in vacuum at 80 °C and calcination in air at 400 °C for 2 h. The MM procedure took place by the following stages: (i) a mixture of cerium hydroxide (synthesized under the conditions described above excluding the calcination step) and the calculated amount of Fe_2O_3 was subjected to mechanical mixing for 30 min in a mortar; (ii) calcination at 400 °C for 2 h. Depending on the preparation method and the Fe_2O_3 content, the supports were denoted as xFeCeIM and xFeCeMM (x = 5, 10 and 20).

Gold catalysts (3 wt%) were prepared by deposition-precipitation method. Prior to the deposition of gold, all Fe-loaded ceria supports were activated in an ultrasound disintegrator. The deposition of gold was carried out by precipitation of $HAuCl_4 \cdot 3H_2O$ with K_2CO_3 under vigorous stirring, while keeping constant pH 7. The precursors were dried under vacuum and calcined in air at 400 °C for 2 h. The gold-containing samples on the mixed supports were denoted as AuxFeCeIM and AuxFeCeMM (x = 5, 10 and 20).

Au/CeO_2 (AuCe) and Au/Fe_2O_3 (AuFe) samples were also prepared and used as references. Hematite, used as support of AuFe, was synthesized by homogeneous coprecipitation method using urea as precipitant. The aqueous solutions of $Fe(NO_3)_3 \cdot 9H_2O$ (Sigma–Aldrich, p.a.) and urea were mixed under vigorous stirring and heated to boiling. Then, the precipitate was aged at 100 °C for 8 h under constant stirring and addition of water. Finally, the precipitate was filtered, washed, dried under vacuum at 80 °C and calcined in air at 400 °C for 2 h.

2.2. Sample characterization

The textural characterization of the samples was performed with a Carlo Erba Sorptomatic 1900 instrument. The fully computerized analysis of the nitrogen adsorption isotherm at −196 °C allowed to estimate the specific surface areas of the samples, through the BET method in the standard pressure range 0.05–0.3 p/p_0. X-ray powder diffraction (XRD) patterns for phase identification were recorded on a Philips PW 1050 diffractometer, equipped with Cu Kα tube and scintillation detector. Data for cell refinements were collected in θ–2θ, step-scan mode in the angle interval from 20 to 110° (2θ), at steps of 0.03° (2θ) and counting time of 3 s/step. The cell refinements were obtained with the PowderCell program [19]. The size – strain analysis was carried out using the BRASS-Bremen Rietveld Analysis and Structure Suite [20].

The temperature programmed reduction (TPR) measurements were carried out by means of an apparatus described elsewhere [21]. A cooling trap (−40 °C) for removing water formed during reduction was mounted in the gas line prior to the thermal conductivity detector. A hydrogen–argon mixture (10% H_2), dried over a molecular sieve 5A (−40 °C), was used to reduce the samples at a flow rate of 24 ml min^{-1}. The temperature was linearly raised

at a rate of $15\,°C\,min^{-1}$. The amount of used sample was 0.05 g. Such amount was selected by the criterion proposed by Monti and Baiker [22]. Hydrogen consumption during the reduction process was calculated using preliminary calibration of the thermal conductivity detector, performed by reducing different amounts of NiO to Ni^0 (NiO – 'analytical grade', calcined at $800\,°C$ for 2 h to avoid the presence of non-stoichiometric oxygen).

Room temperature Mössbauer spectra were obtained by measurements with a Wissel (Wissenschaftliche Elektronik GmbH, Germany) electromechanical spectrometer working in a constant acceleration mode. A $^{57}Co/Rh$ (activity $\cong 50\,mCi$) source and a α-Fe standard were used. The parameters of hyperfine interaction such as isomer shift (δ), quadrupole splitting (Δ), magnetic hyperfine field (B), line widths (FWHM) and relative weight (G) of the partial components in the spectra were determined. Mössbauer spectra of initial samples and samples after catalytic test in NO reduction by CO were registered.

2.3. Catalytic activity measurements

The catalytic test of NO reduction by CO was performed using a quartz glass U-shaped reactor, equipped with a temperature programmed controller. The reactants and products were monitored by ABB IR and UV analyzers. The QM (quadrupole mass) analysis of the reaction products was also performed using on-line Pfeiffer quadrupole mass spectrometer and Balzers Quadstar software. The conversion degree of NO and CO was taken as a measure of catalytic activity. The steady-state tests were made upon increasing the reaction temperature, waiting at each temperature for a constant conversion value. The catalysts were tested at temperatures up to $300\,°C$ at a flow rate of $50\,ml\,min^{-1}$ corresponding to WHSV of $60\,000\,ml\,g^{-1}\,h^{-1}$. The sample's mass was 0.05 g. The pretreatment of the catalyst was provided according to the previously chosen conditions [10,14] using 5% H_2 in argon for 30 min at $120\,°C$. Since the exhaust gases from engines usually contain water vapor and hydrogen, the catalytic activity tests were performed using the gas feed composition 3000 ppm NO + 3000 ppm CO + 1000 ppm H_2 + 5% H_2O (He as balance).

3. Results

3.1. Catalytic behavior in NO reduction by CO

The comparison between temperature dependence of the steady-state activities, expressed as NO and CO conversion, as well as the registered N_2O formation over the gold catalysts on bare ceria, Fe_2O_3 and differently prepared Fe-doped ceria is shown in Fig. 1(a–c). NO_2 was not registered and the amount of CH_4 as a side product presented in some cases was below 2%. It is seen that the gold catalysts on hematite exhibited clearly worst performance in NO reduction by CO as compared to gold on ceria containing samples. In Fig. 1(a) significantly higher NO conversion is observed over gold on Ce–Fe supports as compared to bare ceria, especially in the lower temperature interval below $250\,°C$. The highest NO conversion of about 90% (at $250\,°C$ and above) was reached over gold catalysts on MM supports and Au5FeCeIM sample. The CO conversion degrees (except the data for AuFe) are quite similar (Fig. 1b). The highest CO conversion exhibited Au5FeCeMM (99% at $250\,°C$), followed by AuCe (97%) and Au5FeCeIM (95%). The N_2O formation (Fig. 1c) in the case of IM preparation method was high and quite independent on the Fe-dopant amount. It was comparable with that over AuFe but the highest value of about 60% was attained at lower temperatures (maximum at $100\,°C$ as compared to $250\,°C$ for AuFe). The N_2O was formed up to $200\,°C$ over gold catalysts on
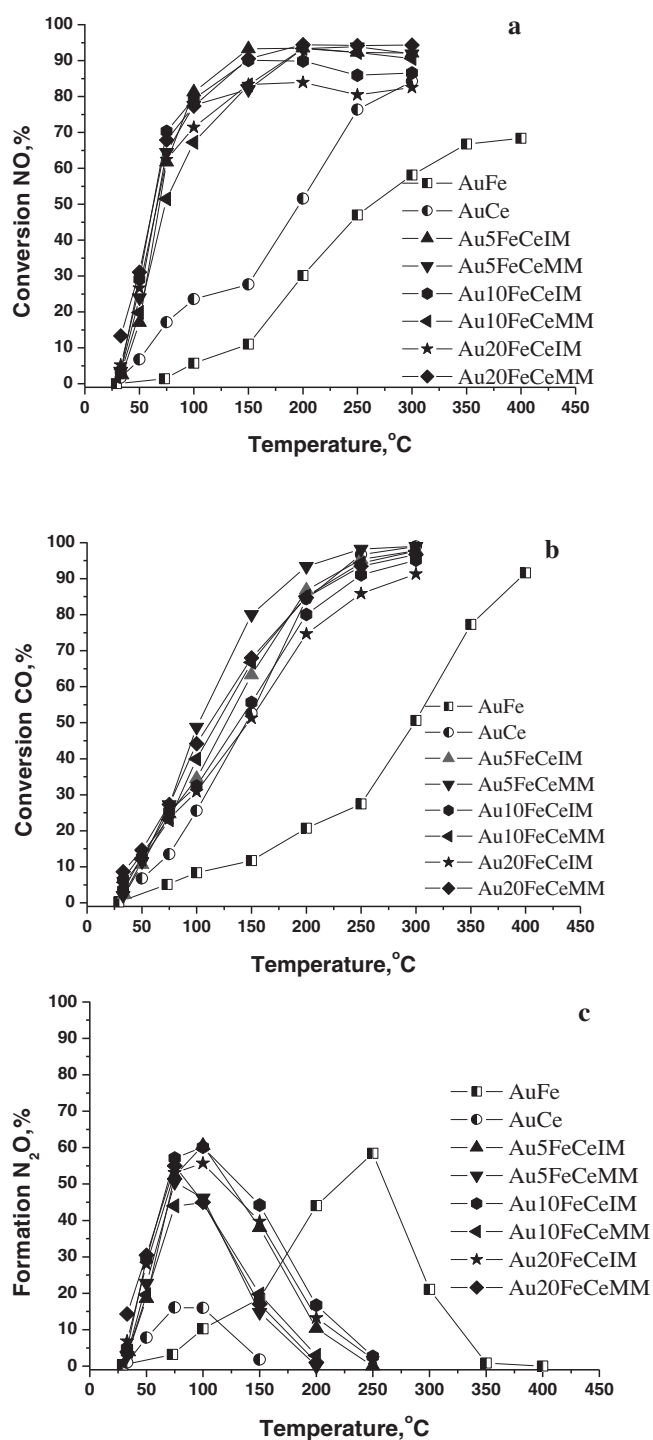

Fig. 1. Temperature dependence of NO (a) and CO conversion (b) as well as N_2O formation (c) over gold catalysts on Fe_2O_3, CeO_2 and Fe-loaded ceria supports prepared by IM and by MM methods.

mixed supports prepared by MM. The amount of N_2O over AuCe was the lowest and it was registered only up to $150\,°C$.

Ammonia is another undesirable side product. The beginning of the NH_3 formation was detected by MS analysis at different temperatures depending on the catalyst's composition. It started above $250\,°C$ over AuCe, Au5FeCeIM and Au10FeCeIM catalysts and above $200\,°C$ over Au20FeCeIM sample, while over the catalysts on MM prepared supports ammonia was already registered above $150\,°C$. Concerning AuFe sample, which is characterized with higher temperature activity, ammonia was observed above $350\,°C$.

Table 1
BET surface area; average size of ceria, Fe_2O_3 and gold particles estimated by XRD.

Sample	S_{BET} ($m^2 g^{-1}$)	Average particles size		
		Gold (nm)	CeO_2 (nm)	Fe_2O_3 (nm)
Au5FeCeIM	99	7.7	7.8	nd
Au10FeCeIM	80	6.9	7.6	nd
Au20FeCeIM	100	6.4	7.9	26.1
Au5FeCeMM	102	nd	7.5	24.2
Au10FeCeMM	90	<3.0	7.7	32.8
Au20FeCeMM	88	nd	7.3	35.8

AuCe: av. size of ceria = 11.5 nm and av., size of gold = 6.8 nm, nd–not detectable

Table 2
Experimental HC ($HC_{exp.}$) in the LT interval of the TPR profiles and the stoichiometric HC needed for ceria surface reduction ($HC_{st.ceria}$) and $Fe_2O_3 \rightarrow Fe_3O_4$ transformation ($HC_{st.iron}$).

Catalyst	$HC_{exp.}$ ($mmol g^{-1}$)	$HC_{st.ceria}$ ($mmol g^{-1}$)	$HC_{st.iron}$ ($mmol g^{-1}$)
AuCe	0.47	0.48–0.58	–
Au5FeCeIM	0.53	0.46–0.55	0.11
Au10FeCeIM	0.55	0.44–0.52	0.21
Au20FeCeIM	0.68	0.39–0.46	0.42
Au5FeCeMM	0.67	0.46–0.55	0.11
Au10FeCeMM	0.71	0.44–0.52	0.21
Au20FeCeMM	0.54	0.39–0.46	0.42

The stability test of Au5FeCeIM catalyst was performed at 250 °C keeping the sample under reaction conditions for 25 h. No changes in NO and CO conversion were registered.

3.2. Sample characterization

3.2.1. XRD measurements

Diffraction lines typical for the face-centered cubic fluorite structure of CeO_2 were registered by XRD measurements of all studied catalysts, while a separate hematite phase was observed for supports synthesized by mechanical mixing and for the Au20FeCeIM sample (see Fig. 2). The close inspection of the typical of metallic Au (1 1 1) reflections at $2\theta = 38.2°$ is shown in Fig. 2b. The Au (1 1 1) reflections were well visible for all IM catalysts. In the case of MM preparation, a weak Au reflection was seen only for the Au10FeCeMM catalyst. The additional presence of hematite (1 1 0) reflections at $2\theta = 35.6°$ (Reference code: 00-033-0664) could be seen.

The average size of gold particles, calculated on the basis of XRD data, given in Table 1, was in the range 6.4–7.7 nm for the supports prepared by IM. As it was mentioned, for MM catalysts with 5 and 20% Fe_2O_3 gold was not detectable, for Au10FeCeMM the Au average particle size was estimated as below 3 nm. In Table 1 are also listed the values of the BET surface area and the average size of CeO_2 and Fe_2O_3 particles. The BET surface area was 80–100 $m^2 g^{-1}$.

The average size of ceria and hematite does not differ significantly being in the frame of 7.3–7.9 nm and 24–36 nm, respectively.

3.2.2. H_2-TPR measurements

In Fig. 3(a and b) the TPR profiles of the studied gold catalysts and AuCe sample are compared in the low temperature (LT) interval up to 350 °C, which is of interest for the reduction of NO by CO. The influenced by gold and by the Fe ions ceria surface layers reduction and the $Fe^{3+} \rightarrow Fe^{2+}$ transition have to be taken into consideration. The end of the LT TPR peaks of gold catalysts on MM supports is about 200 °C, while in the case of IM supports the peaks are much broader and they are completed at higher temperature of about 325 °C. The possible assignment of these LT TPR peaks could be done via comparison between the experimental hydrogen consumption (HC) and the theoretical values of HC for both ceria surface reduction and $Fe_2O_3 \rightarrow Fe_3O_4$ transformation for each support composition. The theoretical HC for ceria surface reduction were calculated having in mind that the reduction, which does not affect the fluorite structure of CeO_2 is limited to 17% [23] or to 20% [24]. The experimental and theoretical HC values are illustrated in Table 2. The data for AuCe are also given for comparison (0.47 mmol g^{-1} corresponding to 16.6% degree of reduction). The reduction of positively charged gold would have a too small HC contribution, as compared to other reduction processes. Separate hematite phase in Au5FeCeIM and Au10FeCeIM catalysts was
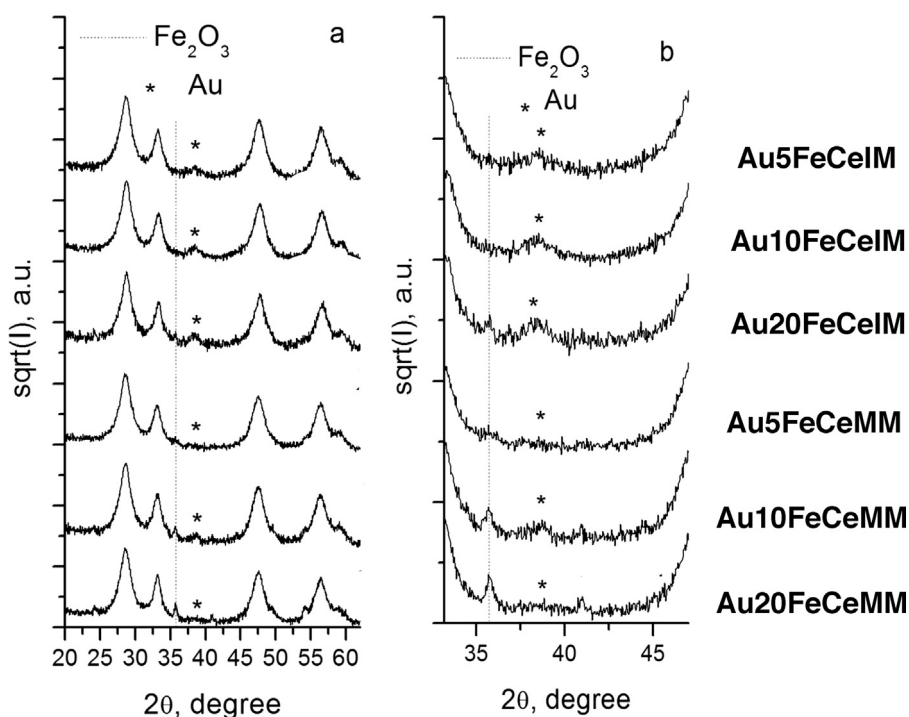

Fig. 2. XRD patterns of the studied gold catalysts on Fe-doped ceria supports (a) and corresponding close inspection of the reflections in the range $2\theta = 34 − 40°$ (b).
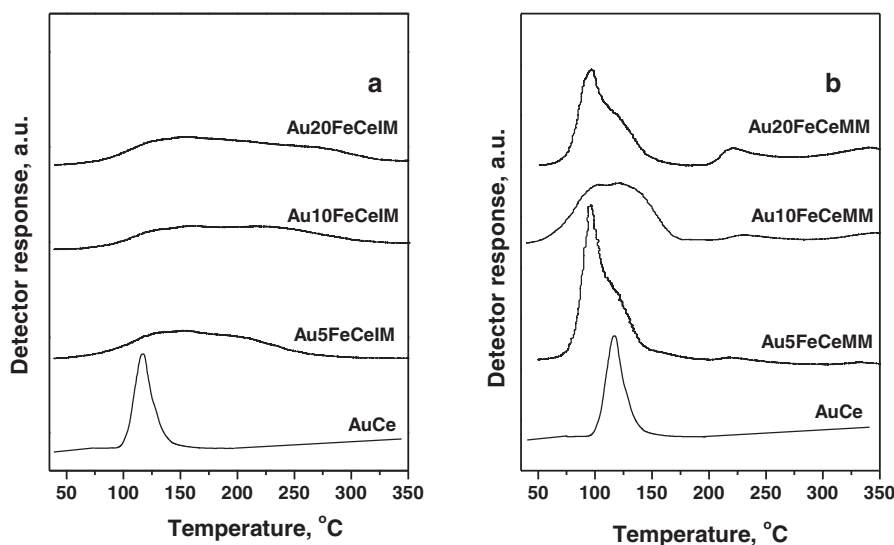
Fig. 3. Comparison between TPR profiles in the LT interval up to 350 °C of gold on ceria and gold on Fe-loaded ceria supports prepared by IM (a) and MM methods (b).

hardly detected by XRD and the HC for the reduction of the existing nano-hematite with low relative weight ($G = 8\%$) [25] can be also neglected.

In the case of Au5FeCeIM catalyst the stoichiometric HC for ceria surface reduction is 0.46–0.55 mmol g^{-1}. Comparing with the obtained experimental value of 0.53 mmol g^{-1}, it could be concluded that the main process up to 325 °C is the ceria surface layers reduction. Only ceria surface reduction can be considered for Au10FeCeIM (stoichiometric HC of 0.44–0.52 mmol g^{-1} for ceria surface reduction and experimental HC of 0.55 mmol g^{-1}) as well. For Au5FeCeMM sample with evidenced separate hematite phase the experimental HC of 0.67 mmol g^{-1} correlates with reduction process (finishing up to 200 °C) of ceria and Fe$_2$O$_3$ → Fe$_3$O$_4$ (total stoichiometric value of 0.57–0.66 mmol g^{-1} for both processes). Applying similar approach of considerations, the reduction of the existing Fe$_2$O$_3$ phase supplementary to surface ceria occurs in the case of Au10FeCeMM sample (the stoichiometric HC for both processes is 0.65–0.73 mmol g^{-1} and experimental HC is 0.71 mmol g^{-1}). Following the same procedure for Au20FeCeMM sample, the reduction processes seem incomplete because the experimental HC value was lower as compared to the theoretically needed. Most probably the higher coverage of hematite phase caused a lower degree of ceria surface reduction hindering the process.

3.3.3. Mössbauer spectroscopy measurements

In Figs. 4 and 5 are illustrated the Mössbauer spectra registered with fresh and used in NO reduction gold catalysts on MM and IM supports, respectively. The spectra involved components without expressed hyperfine splitting (quadrupole doublets, Db), as well as components with magnetic splitting (sextets, Sx). The estimated Mössbauer parameters are listed in Table 3 and Table 4. The parameters for both Sx and Db components are characteristic of high-spin Fe^{3+} ions in octahedral coordination. The parameters of the Sx components evidenced the presence of α-Fe$_2$O$_3$ phase (hematite) with particles size above 10 nm (in accordance with the shown in Table 1 XRD results). For the fresh catalysts on MM supports with different Fe-amount, the hyperfine parameters of the spectral components have similar values, e.g., they do not depend on the content of the iron oxide in the samples. The Db components can be assigned to both a presence of superparamagnetic hematite particles and Fe^{3+} ions incorporated in ceria structure. The very small relative weight ($G \leq 5\%$) of the Db components in the case of MM

preparation method can be related to the predominant surface ceria modification. In the spectra of fresh Au5FeCeIM and Au10FeCeIM samples only Db form was registered, which can be due to the formation of Ce$_{1-x}$Fe$_x$O$_2$ solid solutions. In addition to the Db with $G = 76\%$, the presence of Sx due to a separate hematite phase (registered by XRD as well) was found with Au20FeCeIM sample. The high relative weight of Db components in the case of IM samples reveals bulk ceria modification caused by this method of support's preparation.

After catalytic tests in NO reduction by CO (final temperature of 300 °C), a tendency of increasing of Sx and lowering Db relative part was seen. This could be explained by agglomeration of ultrafine superparamagnetic hematite particles to particles with average size above 10 nm. Interesting observation is the fact that for used catalysts the single sextet of hematite as in the initial samples was kept. No transformation in the spectra characteristic for the partial reduced Fe ions of different valence and coordination state was observed.

4. Discussion

The catalytic tests over the studied gold catalysts (Fig. 1) clearly showed that the Fe-modification of ceria is beneficial especially for NO conversion. It should be stressed the remarkable difference below 250 °C in the CO and NO conversion values for the gold on bare ceria. It could be explained supposing that the registered CO conversion is not only due to the NO + CO interaction but to a supplemental process – most probable the water gas shift reaction (WGSR); the gas stream does not contain O$_2$ and the low temperature CO oxidation by the participation of less mobile at these conditions lattice oxygen is amazing. The results for gold catalysts on mixed supports prepared by different methods and containing various Fe-amounts did not differ significantly. On the basis of similar high activities of the catalysts on MM supports and Au5FeCeIM sample it could be concluded that for the reduction of NO by CO: (i) The high gold dispersion is not a crucial factor as the gold particles on MM prepared mixed supports were very small, while lower gold dispersion (7.7 nm, see Table 1) was observed for Au5FeCeIM. This statement is in agreement with a previous study by FTIR revealing that the presence of gold was not related to the generation of intermediate isocyanates (NCO) species. It was found that gold plays an important role in the generation of oxygen vacancies but the effect of gold particles size does not seem of great importance [16]; (ii)
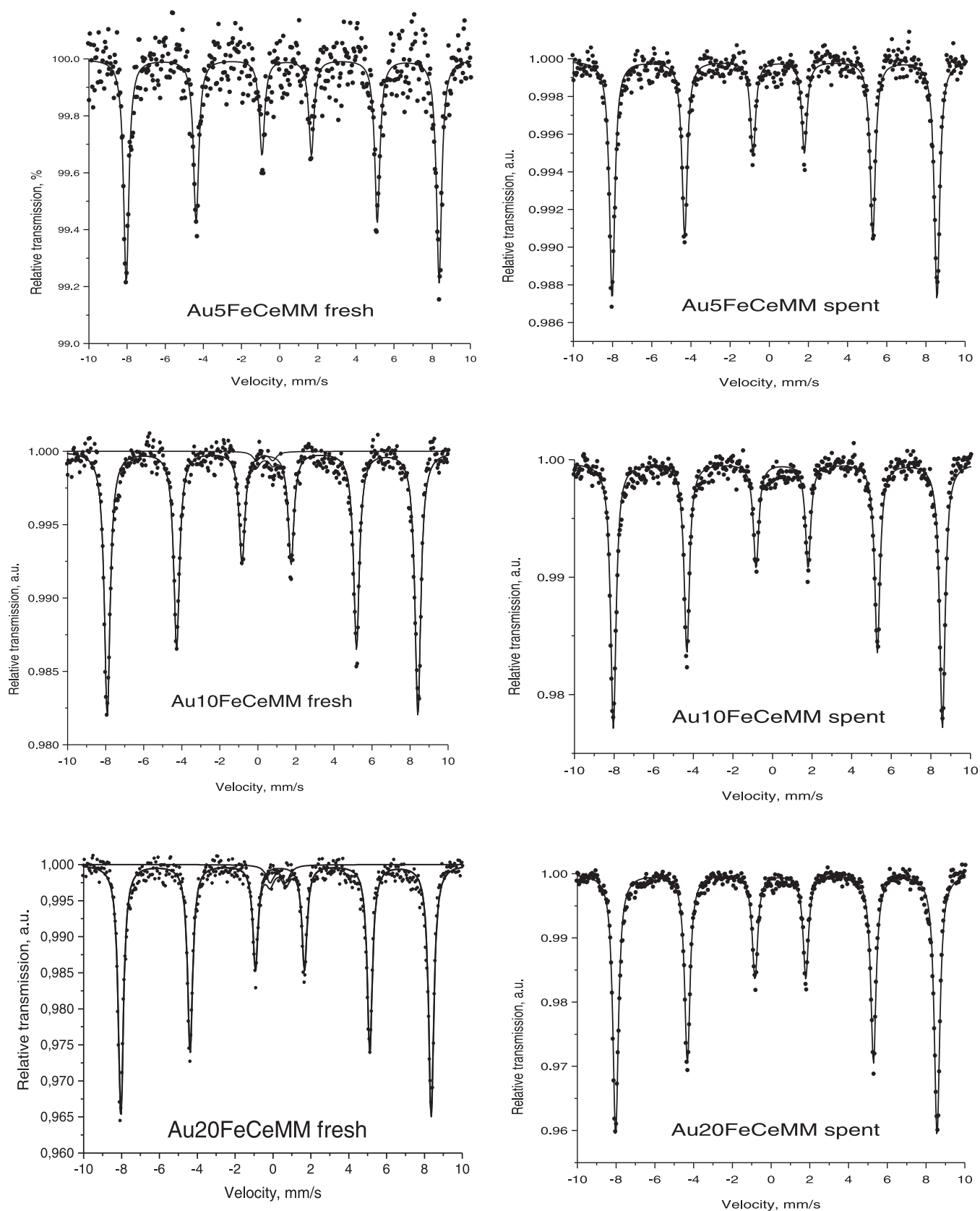
Fig. 4. Mössbauer spectra of fresh and spent gold catalysts on Ce–Fe supports prepared by MM method.
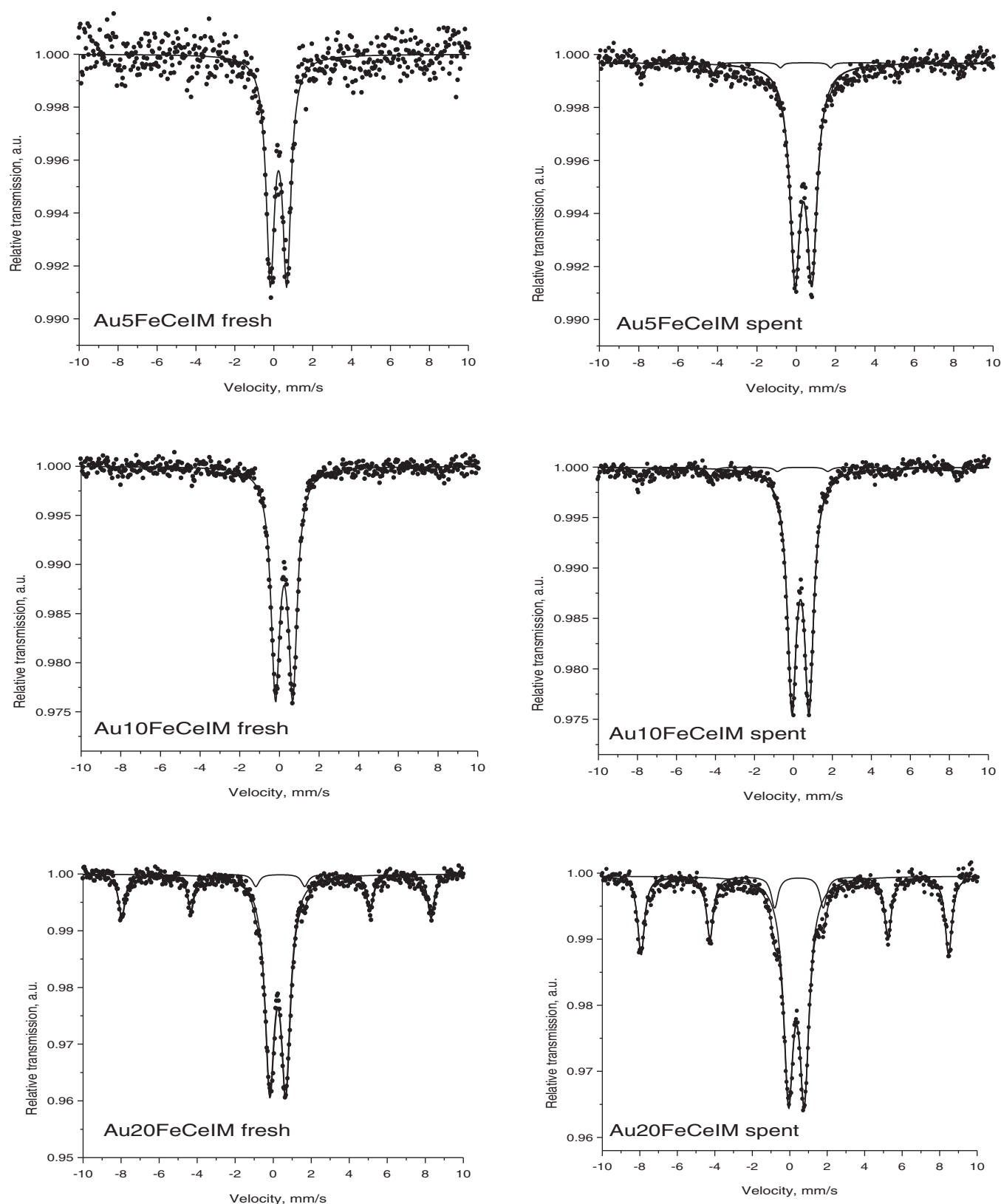
Fig. 5. Mössbauer spectra of fresh and spent gold catalysts on Ce–Fe supports prepared by IM method.

The modification of ceria by incorporation of lower Fe^{3+} amount like in Au5FeCeIM and in the case of MM preparation (Mössbauer results of small relative weight of Db components) is beneficial.

It is interesting to distinguish the role of Fe addition. On one hand it is a ceria modifier but a separate hematite phase could

also play a role. It was mentioned above that the positive role of Fe-doping is related mainly to NO conversion. However, concerning $DeNO_x$ not only the activity but also the selectivity to N_2 is a key factor. The amount of registered N_2O over the studied gold catalysts on Fe-doped ceria was bigger and N_2O was registered up to

Table 3
Parameters evaluated from the Mossbauer spectra of the studied fresh and used in NO reduction gold catalysts on MM supports.

Sample	Components	δ (mm/s)	Δ (mm/s)	B (T)	FWHM (mm/s)	G (%)
Au5FeCeMM fresh	$Sx - \alpha - Fe_2O_3$	0.37	−0.11	51.0	0.33	100
Au5FeCeMM spent	Sx	0.37	−0.21	51.5	0.33	100
Au10FeCeMM fresh	Sx	0.35	−0.21	50.8	0.37	98
	Db	0.36	0.84	–	0.48	2
Au10FeCeMM spent	Sx	0.38	−0.21	51.6	0.33	100
Au20FeCeMM fresh	$Sx - \alpha - Fe_2O_3$	0.37	−0.10	51.0	0.33	95
	$Db - Fe^{3+}$	0.37	0.83	–	0.50	5
Au20FeCeMM spent	Sx	0.38	−0.21	51.5	0.34	100

higher temperatures than in the case of AuCe sample. The amount of N_2O on supports prepared by IM was higher as compared to MM supports (Fig. 1c).

The different preparation methods reflect on the support's structure. The mixed supports prepared by MM method consist of ceria with slight surface modification during mechanochemical activation (relative part $G \leq 5\%$ for Db components) and separate hematite phase evidenced both by XRD and Mössbauer data. Some amount of not detectable by XRD nano-hematite is evidenced by HRTEM observations and Mössbauer results at LNT [25]. In the case of IM method the Mössbauer results reveal $Ce_{1-x}Fe_xO_2$ solid solution (deeper ceria modification by Fe^{3+} insertion). The TPR results of Au5FeCeIM and Au10FeCeIM catalysts in the temperature interval of NO reduction tests showed that mainly the surface reduction of Fe-modified ceria phase took place (the contribution of the reduction of the small amount of nano-hematite is negligible). The role of ceria for NO dissociation is well known. Trovarelli et al. [26] have established that NO adsorbs onto ceria which promotes NO desorption as N_2 at much lower temperatures than ceria-free samples. The NO + CO study over CeO_2, Au/CeO_2 and $Au/CeO_2-Al_2O_3$ catalysts was carried out by some of us by means of FTIR [16]. The NCO species formed by a process involving the dissociation of NO on the oxygen vacancies of the ceria support, followed by the reaction between the N atoms lying on the surface and the CO molecules was evidenced. By this way the catalytic activity was associated with the formation of oxygen vacancies during the contact of the reacting gases, NO, CO and H_2, with the catalyst surface. The NCO species were detected on all of the samples and a conclusion was drawn that they were generated on oxygen deficient sites on ceria supports independent on the presence of gold. However, as it was already discussed above, gold plays an important role in the modification of ceria favorable for surface oxygen vacancies formation in a significantly lower temperature range [16].

A reaction scheme showing the possibility for N_2O formation at the beginning of the process of CO reduction by H_2 over CeO_2 has been proposed by Daturi et al. [27]. The scheme includes NO dissociation as two oxygen atoms from two NO molecules fill two neighboring oxygen vacancies re-oxidizing the pre-reduced ceria surface, while the nitrogen atoms recombine giving rise to a N_2 molecule. The authors have suggested that above 250–300 °C the nitrogen protoxide is not more registered either because of its reduction by H_2 or by acting as re-oxidizing agent for the reduced surface by trapping oxygen in a vacancy. In our case the N_2O was produced over gold on bare ceria only up to 150 °C. The Fe- loading of CeO_2 increased the N_2O amount as well as the temperature range of its formation, more markedly using IM preparation method. The explanation could be that for catalysts on MM supports free of hematite ceria surface exists, while in the case of IM supports the nano-hematite phase, covering the ceria grains [25], could be responsible for the higher N_2O initiation. The fact that Fe_2O_3 is one of the catalysts over which N_2O formation is favored has long been established. Sugi et al. [28] have explained the N_2O formation at an early stage of the NO reduction over Fe_2O_3 by the difference in adsorptivity between NO and N_2O – the adsorption of NO is stronger than that of N_2O. The authors associated the dependence of N_2O formation on the temperature by the following way: at the beginning of the reduction process, adsorption equilibrium between NO and N_2O is established and N_2O is displaced by NO before it is converted to N_2; as the temperature is raised, a part of the N_2O formed on the catalyst will be reduced to N_2 before the displacement by NO.

The conducted Mössbauer measurements, especially of used catalysts, were addressed in particular to clarify the participation of the Fe-phase in the reaction of NO reduction by CO. On the bases of the observed reducibility of the gold catalysts, confirmed by the evaluated values of HC, the participation of the existing separate hematite phase in the redox processes was expectable. Investigating the reduction of N_2O and NO by CO under transient conditions,

Table 4
Parameters evaluated from the Mossbauer spectra of the studied fresh and used in NO reduction gold catalysts on IM supports.

Sample	Components	δ (mm/s)	Δ (mm/s)	B (T)	FWHM (mm/s)	G (%)
Au5FeCeIM fresh	$Db - Fe^{3+}$	0.35	0.84	–	0.51	100
Au5FeCeIM spent	Sx	0.37	−0.21	50.3	0.31	7
	Db	0.37	0.86	–	0.63	93
Au10FeCeIM fresh	$Db - Fe^{3+}$	0.35	0.87	–	0.54	100
Au10FeCeIM spent	Sx	0.37	−0.21	50.8	0.40	8
	Db	0.37	0.88	–	0.56	92
Au20FeCeIM fresh	$Sx - \alpha - Fe_2O_3$	0.38	−0.11	50.6	0.42	24
	$Db - Fe^{3+}$	0.34	0.84		0.59	76
Au20FeCeIM spent	Sx	0.38	−0.22	51.0	0.44	37
	Db	0.36	0.84	–	0.63	63

Randall et al. [29] have proposed that on Fe_2O_3 CO is oxidized to CO_2 and the catalyst is reduced to Fe_3O_4; N_2O and N_2 are formed by the reaction of NO and N_2O with surface oxygen vacancies, and the catalyst is thus re-oxidized to Fe_2O_3. The authors have shown that the composition of the catalyst changes during relaxation to steady-state, where it reaches a rather reduced state, close to Fe_3O_4. However, at the present reaction conditions no transformation into two sextets with parameters characteristic of magnetite was evidenced for the gold catalysts on Fe-loaded ceria used in CO + NO reaction up to 300 °C. The possible role of hematite as co-catalyst in NO + CO reaction could be eventually explained by the participation of Fe_2O_3 clusters as proposed on the basis of DFT calculations [30]. The authors suggested that CO or NO adsorbed on the Fe_2O_3 weakens one of the O—Fe bonds to create a loosely attached O site. A subsequent CO gets oxidized by this O transforming the cluster to Fe_2O_2; NO is reduced via multiple oxidation and reduction steps that return the cluster to the oxidized Fe_2O_3 state.

Ammonia is an undesirable side product as a toxic air pollutant. On one hand NH_3 could be formed by the interaction between NO and H_2 used as a component of the gas stream. The water in the feed could further increase the H_2 concentration by WGSR. On the other hand it is known that NCO groups formed on various oxides easily hydrolyze to ammonia in the presence of water [31–33]. The amount of ammonia registered during the present experiments increased at higher temperatures. Obviously ammonia could not act as effective reducing agent of NO under the conditions used.

Comparing NO reduction by CO over the studied gold catalysts on Fe-loaded ceria, the most promising results were obtained with Au5FeCeIM sample at 250 °C: high catalytic activity of 92% NO conversion and 95% CO conversion and 100% selectivity toward N_2 at this temperature.

5. Conclusion

The study showed that gold catalysts on ceria and Fe- loaded ceria exhibited clearly better performance in NO reduction by CO as compared to gold on Fe_2O_3. The Fe- modification of ceria was beneficial especially for NO conversion. On the basis of similar high activities of the catalysts on MM supports and Au5FeCeIM sample, it was concluded that concerning the reduction of NO by CO the presence of very small gold particles is not of crucial importance and the ceria modification by incorporation of lower Fe^{3+} amount is beneficial. However, the Fe-doping decreased the selectivity to N_2 by increasing the selectivity to N_2O.

The observed high catalytic activity, the 100% selectivity to N_2 and good stability during the reduction of NO by CO at 250 °C over Au5FeCeIM make this gold catalysts promising for practical application in particular during the "cold start" period of the engines.

References

[1] S.A.C. Carabineiro, D.T. Thompson, Gold catalysis, in: C. Corti, R. Holliday (Eds.), Gold Science and Applications, CRC Press, 2009, pp. 89–123.
[2] T. Salama, R. Ohnishi, T. Shido, M. Ichikawa, J. Catal. 162 (1996) 169–178.
[3] A. Ueda, M. Haruta, Gold Bull. 32 (1999) 3–11.
[4] M.C. Kung, J.-H. Lee, H.H. Kung, Am. Chem. Soc. Div. Fuel Chem. 40 (1995) 1073–1081.
[5] M.A.P. Dekkers, M.J. Lippits, B.E. Nieuwenhuys, Catal. Today 54 (1999) 381–390.
[6] J.R. Mellor, A.N. Palazov, B.S. Grigorova, J.F. Greyling, K. Reddy, M.P. Letsoalo, J.H. Marsh, Catal. Today 72 (2002) 145–156.
[7] E. Seker, E. Gulari, Appl. Catal. A 232 (2002) 203–217.
[8] A.C. Gluhoi, S.D. Lin, B.E. Nieuwenhuys, Catal. Today 90 (2004) 175–182.
[9] G.S. Zafiris, R.J. Gorte, J. Catal. 139 (1993) 561–567.
[10] L. Ilieva, G. Pantaleo, I. Ivanov, A.M. Venezia, D. Andreeva, Appl. Catal. B 65 (2006) 101–109.
[11] L. Ilieva, G. Pantaleo, I. Ivanov, R. Nedyalkova, A.M. Venezia, D. Andreeva, Catal. Today 139 (2008) 168–173.
[12] L. Ilieva, G. Pantaleo, J.W. Sobczak, I. Ivanov, A.M. Venezia, D. Andreeva, Appl. Catal. B 76 (2007) 107–114.
[13] L. Ilieva, G. Pantaleo, R. Nedyalkova, J.W. Sobczak, W. Lisowski, M. Kantcheva, A.M. Venezia, D. Andreeva, Appl. Catal. B 90 (2009) 286–294.
[14] L. Ilieva-Gencheva, G. Pantaleo, N. Mintcheva, I. Ivanov, A.-M. Venezia, D. Andreeva, J. Nanosci. Nanotechnol. 8 (2008) 867–873.
[15] M.M. Mohamed, T.M. Salama, M. Ichikawa, J. Colloid Interface Sci. 224 (2000) 366–371.
[16] M. Kantcheva, O. Samarskaya, L. Ilieva, G. Pantaleo, A.M. Venezia, D. Andreeva, Appl. Catal. B 88 (2009) 113–126.
[17] M. Shelef, H.S. Gandhi, Ind. Eng. Chem. Prod. Res. Dev. 11 (1) (1972) 2–11.
[18] A. Gupta, U. Waghmare, M. Hegde, Chem. Mater. 22 (2010) 5184–5198.
[19] W. Kraus, G. Nolze, PowderCell for Windows, version 2.4; Federal Institute for Materials Research and Testing, 5, Rudower Chaussee, Berlin, Germany, 2000, pp. 12489.
[20] J. Birkenstock, R.X. Fisher, T. Messner, BRASS 2003: the Bremen Rietveld analysis and structure suite. Ber. DMG, Beih. z, Eur. J. Mineral. 15 (1) (2003) 21–28.
[21] N. Kotzev, D. Shopov, J. Catal. 22 (1971) 297–301.
[22] D.A.M. Monti, A. Baiker, J. Catal. 83 (1983) 323–335.
[23] M.G. Sanchez, J.L. Gazquez, J. Catal. 104 (1987) 120–135.
[24] A. Laachir, V. Perrichon, A. Bardi, J. Lamotte, E. Catherine, J.C. Lavalley, J. El Faallah, L. Hilaire, F. Le Normand, E. Quemere, G.N. Sauvion, O. Touret, J. Chem. Soc. Faraday Trans. 87 (1991) 1601–1609.
[25] L. Ilieva, T. Tabakova, G. Pantaleo, I. Ivanov, R. Zanella, D. Paneva, N. Velinov, J.W. Sobczak, W. Lisowski, G. Avdeev, A.M. Venezia, Appl. Catal. A 467 (2013) 76–90.
[26] A. Trovarelli, C. de Leitenburg, M. Boaro, G. Dolcetti, Catal. Today 50 (1999) 353–367.
[27] M. Daturi, N. Bion, J. Sassey, J.-C. Lavalley, C. Hedoin, T. Seguelong, G. Blanchard, Phys. Chem. Chem. Phys. 3 (2001) 252–255.
[28] Y. Sugi, N. Todo, T. Sato, Bull. Chem. Soc. Jpn. 48 (1975) 337–338.
[29] H. Randall, R. Doepper, A. Renken, Appl. Catal. B 17 (1998) 357–369.
[30] B.V. Reddy, S.N. Khanna, Phys. Rev. Lett. 93 (6) (2004) 68,301-1–68,301-4.
[31] F. Solymosi, T. Bansagi, J. Phys. Chem. 83 (1979) 552–553.
[32] F. Poignant, J. Saussey, J.C. Lavalley, G. Mabilon, Chem. Commun. (1995) 89–90.
[33] Y.H. Yeom, B. Wen, W.M.H. Sachtler, E. Wetz, J. Phys. Chem. B 108 (2004) 5386–5404.